APPLICATION OF MOLECULAR MACHINES IN PHOTOELECTROCHEMISTRY

Mirela I. Iorga[1], Mihai V. Putz[1, 2,(*)]

1. Laboratory of Renewable Energies-Photovoltaics, R&D National Institute for Electrochemistry and Condensed Matter –INCEMC–Timisoara
2. Laboratory of Structural and Computational Physical-Chemistry for Nanosciences and QSAR, Biology-Chemistry Department, West University of Timisoara
(*) Correspondent author: MVP: mv_putz@yahoo.com, mihai.putz@e-uvt.ro

Abstract
The paper presents an original integrated photo-electro-chemistry algorithm developed by the authors for the possibilities of application of molecular machines in photoelectrochemistry. Concerning molecular machines, five main directions have been approached: the representation of the studied system through computational programs, the calculation of reaction parameters based on HSAB principle, estimation of Coulomb blockade, predictions on the bondonic photovoltaic effect by bondonic spectral correlations, calculations of the thermodynamic indices of interconversion through the path integral formalism, and estimations about the corresponding binary logical systems.

Introduction
The current trend is to reduce as much as possible the size and weight of parts of devices and machines, with the aim of performing more and more complicated operations with much smaller pieces [1]. Through the combination between the high precision of chemical synthesis and engineering ingenuity, the "bottom-up" molecule-to-molecule approach offers unlimited opportunities for the design and construction of supramolecular nanoscale structures [2].
The design and construction of prototypes [1, 3] for molecular devices, machines and motors is based on natural processes and systems and brings together various branches of science such as supramolecular chemistry, engineering or the latest breakthroughs of synthetic chemistry. The vast majority of engineered molecular machines so far is based on interconnected molecular species such as rotaxanes, catenane and related species [4, 5, 6, 7].
The essential features of rotaxanes and catenanes derive from non-covalent interactions between their components that contain complementary recognition centers. Rotaxanes are prototypes suitable for the construction of both linear and rotary molecular machines. The typical implementation of rotaxanes for molecular machines is the development of molecular shuttles with ring translational movements [8, 9]. This type of molecular machines has a well-organized structure and has to function as multicomponent systems with a proper functional integration [3, 10].
The major importance of such systems is also confirmed by the fact that in 2016 the *Nobel Prize for Chemistry* was awarded to researchers Jean-Pierre Sauvage, Sir J. Fraser Stoddart and Bernard L. Feringa "for the design and synthesis of molecular machines" [11].

Results and discussions
In the present paper the [2]rotaxane $1H^{3+}$ [12, 13] was chosen as the working system, consisting of a dibenzo[24]crown-8 ether (DB24C8), a π-electron-donor macrocycle, and a dumbbell component containing a secondary ammonium center ($-NH_2^+-$) and a 4,4'-bipyridinium (bpy^{2+}) unit. The stoppers are an anthracene moiety on one side and a 3,5-di-tert-butylphenyl group on the other side. Because the charge-transfer (CT) interaction of the p-electron-donor macrocycle with the p-electron-acceptor bpy^{2+} unit is much weaker than the

[N^+-H···O] hydrogen-bonding interactions between the DB24C8 macrocycle and the ammonium center, the [2]rotaxane $1H^{3+}$ will have the stable co-conformation [14] when the macrocycle surrounds the ammonium station, as represented in **Figure 1** by the $1AH^{3+}$ structure. If a base is added, in this case, tributylamine, the ammonium center is converted into an amine function, and the transient state $1A^{2+}$, after the displacement of the macrocycle onto the bpy^{2+} unit is transformed into a stable state $1B^{2+}$. The reverse process can take place if an acid is added, in this case, trifluoroacetic acid, and the system goes to the initial state through the transient state, $1BH^{3+}$. In the case of the deprotonated rotaxane, through one-electron reduction of the bipyridinium unit, the CT interactions are destroyed, and the macrocyclic ring can be displaced from the bpy^{2+} station.

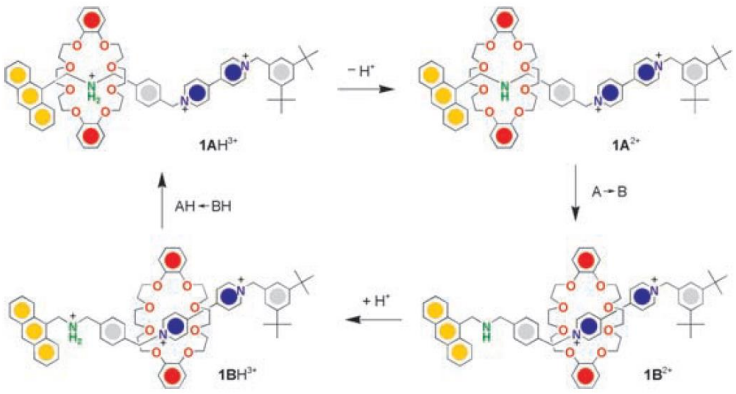

Figure 1. Schematic representation of the shuttling processes of the crown ether ring upon deprotonation and reprotonation of the ammonium site [13]

The structures of the studied rotaxane (initial, transient and final) during the molecular shuttling process were represented in HyperChem and are presented in **Figure 2**.

Based on the "Hard and Soft Acids and Bases" (HSAB) principle, chemical reactivity, transfer energy, and other parameters are calculated. HSAB principle is an important conceptual principle to treat the molecular binding and reactive processes. Writing the energy variation at transfer under the following forms:

$$\Delta E = \Delta\Omega_A + \Delta\Omega_B \quad (1)$$

$$\Delta\Omega_A = -\frac{\eta_A}{4(\eta_A+\eta_B)^2}(\Delta\chi)^2 \quad (2)$$

$$\Delta\Omega_B = -\frac{\eta_B}{4(\eta_A+\eta_B)^2}(\Delta\chi)^2 \quad (3)$$

$$\Delta\chi = \chi_A - \chi_B \quad (4)$$

the optimal energetic transfer will imply, for instance, the minimization of $\Delta\Omega_A$ respecting η_A, in conditions in which $\Delta\chi$ and η_B are maintained constant.

Therefore, the condition to achieve the optimum transfer results to be: $\eta_A = \eta_B$ implying the fact that the species with a high chemical hardness prefer the coordination with species that are high in their chemical hardness, and respectively the species with low softness (the inverse of the chemical hardness) will prefer reactions with species that are low in their softness.

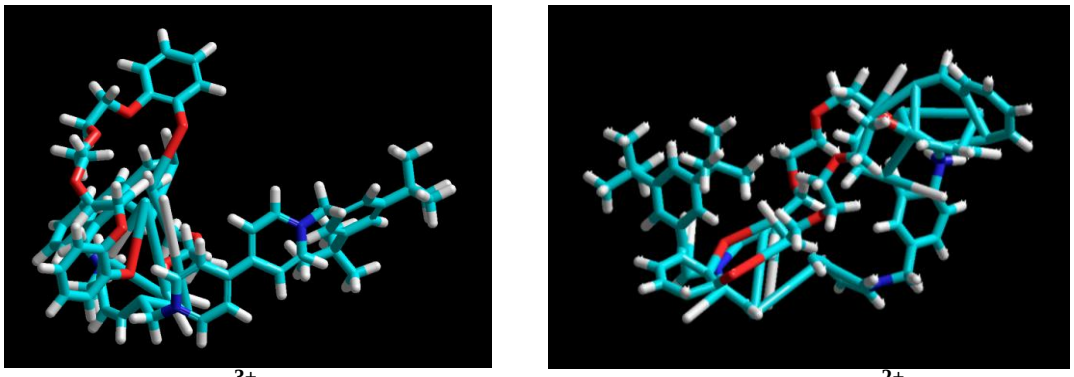

$1AH^{3+}$ $1A^{2+}$

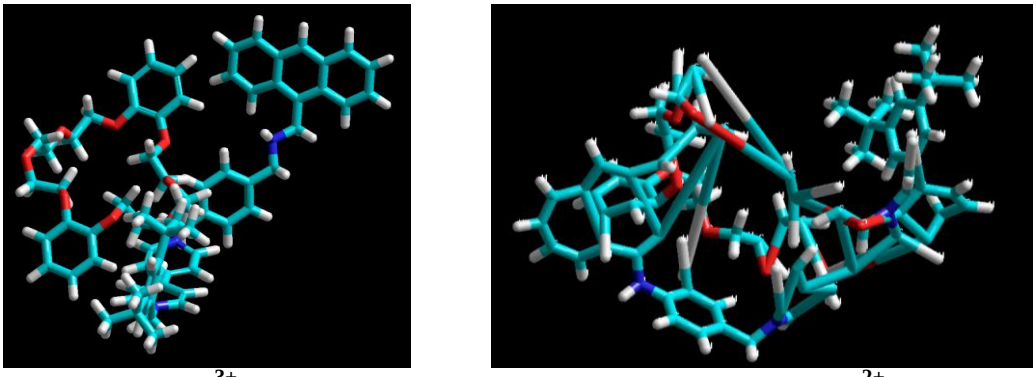

$1BH^{3+}$ $1B^{2+}$

Figure 2. HyperChem representation of the structures (initial, transient and final) of the studied rotaxane during the molecular shuttling process

Coulomb blockade is estimated for these systems. A schematic representation of the Coulomb blockade is given in **Figure 3**. Tunneling/redistribution of electrical charge is expressed by a change in the electrostatic potential. Coulomb blockade allows precise control of a small number of electrons with essential applications in low power dissipation switching devices and thus an increase in the circuit integration level.

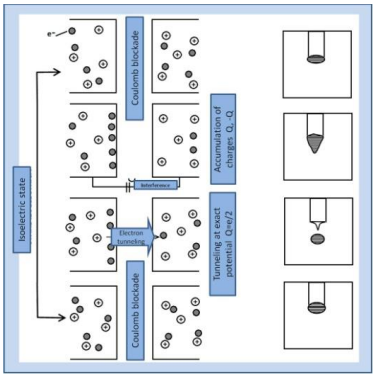

Figure 3. Schematic representation of the Coulomb blockade

Through bondonic spectral correlations, predictions are made on the bondonic photovoltaic effect. The bondonic energy in photovoltaic system due to the Planck quantification is:

$$E_B = \sqrt{hI_{SC} \times V_{OC}} = \hbar \sqrt{\frac{2\pi}{IQ}} \left(18.8177 \times 10^{10}\right) \times \Delta\tilde{\upsilon}_{FWHM}[cm^{-1}] \qquad (5)$$

$$X_B^0[A] = \frac{4.19399 \times 10^6}{E_B[eV]} = 0.0135084 \times 10^{12} \frac{\sqrt{IQ}}{\Delta\tilde{\upsilon}_{FWHM}[cm^{-1}]} \qquad (6)$$

and eventually rewritten into a macroscopic observable scale

$$X_B[meters] = 1.35084 \frac{\sqrt{IQ}}{\Delta\tilde{\upsilon}_{FWHM}[cm^{-1}]} \quad (7)$$

The PV-related bondonic quantum current will be:

$$I_B[A] = \frac{e_B}{t_B} = 1.51146 \times 10^{-7} \frac{\Delta\tilde{\upsilon}_{FWHM}[cm^{-1}]}{IQ^{3/2}} \quad (8)$$

Through the path integral formalism, the thermodynamic indices of interconversion (free energy, enthalpy, entropy, Gibbs energy, etc.) are calculated. The partition function is given as a simple integral:

$$Z_1 = \int_{-\infty}^{+\infty} \frac{dx_0}{\sqrt{2\pi\hbar^2\beta/m_0}} \exp[-\beta W_1(x_0)] \quad (9)$$

In terms of free energy: $F = -\beta^{-1} \log Z$ (10)

$$\Delta G = \frac{1}{\beta} \ln Z - \int \nabla V(x) dx \quad (11)$$

$$\Delta S = \frac{1}{T} \int \nabla V(x) dx \quad (12)$$

Molecular systems convert the input stimulus (optical, electrical or chemical) into output signals (which may also be of optical, electrical or chemical nature). Through the similarity between molecular machines and binary logic systems, represented in **Figure 4**, the quantum logical information is provided, and the type of logical system (AND, OR, XOR) corresponding to every state of the molecular machine during the shuttle movement could be estimated.

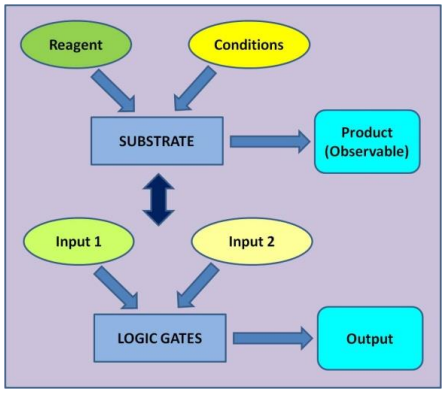

Figure 4. Schematic representation of the similarity between molecular machines and binary logic systems

Conclusion

The five main directions elaborated by the authors of the present paper lead to the development of an integrated photo-electro-chemistry algorithm of molecular machines towards moletronics and smart functionalized nano-materials.

Acknowledgments:

This contribution is part of the Nucleus-Programme under the project "Deca-Nano-Graphenic Semiconductor: From Photoactive Structure to the Integrated Quantum Information Transport" PN-18-36-02-01/2018 funded by the Romanian Ministry of Research and Innovation (MCI). The authors declare no conflict of interest.

REFERENCES

1. Balzani, V.; Credi, A.; Venturi, M. Molecular devices and machines, *Nanotoday*, **2007**, *2*, 18-25.
2. Venturi, M.; Iorga, M.; Putz, M.V. Molecular Devices and Machines: Hybrid Organic-Inorganic Structures, *Current Organic Chemistry*, 2017, *21*, 2731-2759.
3. Balzani, V.; Credi, A.; Venturi, M. *Molecular Devices and Machines. Concepts and Perspectives for the Nanoworld*, Wiley-VCH, Weinheim, **2008a**.
4. Balzani, V.; Credi, A.; Raymo, F.M.; Stoddart, J.F. Artificial molecular machines, *Angew. Chem. Int. Ed.*, **2000**, *39*, 3348-3391.
5. Sauvage, J.P.; Dietrich-Buchecker, C. (Eds.), *Molecular Catenanes, Rotaxanes and Knots*, Wiley-VCH, Weinheim, **1999**.
6. Abendroth, J.M.; Bushuyev, O.S.; Weiss, P.S.; Barrett, C.J. Controlling motion at the nanoscale: rise of the molecular machines, *ACS Nano*, **2015**, *9*, 7746-7768.
7. Venturi, M.; Credi, A. Electroactive [2]catenanes, *Electrochim. Acta*, **2014**, *140*, 467-475.
8. Bissell, A.; Cordova, E.; Kaifer, A.E.; Stoddart, J.F. A chemically and electrochemically switchable molecular shuttle, *Nature*, **1994**, *369*, 133-137.
9. Arduini, A.; Bussolati, R.; Credi, A.; Pochini, A.; Secchi, A.; Silvi, S.; Venturi, M. Rotaxanes with a calix[6]arene wheel and axles of different length. Synthesis, characterization, and photophysical and electrochemical properties, *Tetrahedron*, **2008**, *64*, 8279-8286.
10. Balzani, V.; Credi, A.; Venturi, M. Molecular machines working on surfaces and at interfaces, *Chem. Soc. Rev.*, **2008b**, *9*, 202-220.
11. ***, MLA style: "The Nobel Prize in Chemistry 2016". *Nobelprize.org.* Nobel Media AB 2014. Web. 1 Nov **2016**. http://www.nobelprize.org/nobel_prizes/chemistry/laureates/2016/
12. Ashton, P.R.; Ballardini, R.; Balzani, V.; Baxter, I.; Credi, A.; Fyfe, M.; Gandolfi, M.T.; Gomez-Lopez, M.; Martinez-Diaz, V.; Piersanti, A.; Spencer, N.; Stoddart, J.F.; Venturi, M.; White, A.J.P.; Williams, D.J. Acid-Base Controllable Molecular Shuttles, *J. Am. Chem. Soc.* **1998**, *120*, 11932-11942.
13. Garaude, S.; Silvi, S.; Venturi, M.; Credi, A.; Flood, A.H.; Stoddart, J.F. Shuttling Dynamics in an Acid–Base-Switchable [2]Rotaxane, *ChemPhysChem*, **2005**, *6*, 2145-2152.
14. Fyfe, M.C.T.; Glink, P.T.; Menzer, S.; Stoddart, J.F.; White, A.J.P.; Williams, D.J. Anion-assisted self-assembly, *Angew. Chem. Int. Ed. Engl.*, **1997**, *36*, 2068-2070.